

Glacier flow estimation by SAR image correlation

Fumihiko Nishio

Chiba University

1-33 Yayoi-cho, Inage-ku, Chiba, 263-8522 Japan
fnishio@ceres.cr.chiba-u.ac.jp

Hiroyuki Wakabayashi

Japan Aerospace Exploration Agency

2-4-1 Hamamatsu-cho, Minato-ku, Tokyo 105-8060 Japan
hirowaka@d8.dion.ne.jp

Abstract—The Shirase Glacier is the largest in the Lutzow Holm Bay and is well known as the fastest-flowing ice stream in Antarctica. Although several attempts have been made to measure ice flow velocities of the glacier using ground measurements and remotely sensed data, continuous measurement over a long period has been impossible due to severe environmental conditions and the lack of datasets from continuous observation. This report of our preliminary ice-flow estimations of the Shirase Glacier correlates the amplitude images with the available Synthetic Aperture Radar (SAR) data. We propose to determine ice-flow velocities using this image correlation. We apply our technique to the SAR data obtained by observing the Shirase Glacier to determine and analyze the ice flow velocities in the summary.

Keywords- *ers-2, SAR, image correlation, glacier flow, Shirase Glacier*

I. INTRODUCTION

The Shirase Glacier, located about 100 km south of Syowa Station, is the largest glacier in the Lutzow Holm Bay, as shown in Fig. 1. It is one of the fastest-flowing ice streams in Antarctica with an observed flow velocity of 2.5 km per year [1]. Ice streams are fast-flowing currents of ice that feed the ice shelves or reach the sea at their terminus, thereby controlling the discharge flux of the ice sheet. Many attempts have been made to measure the flow velocities of ice streams because the information is essential in understanding the mass balance of the ice sheet. The tools used in these attempts were Global Positioning System (GPS) receivers, video images taken by interval camcorders, and aerial photographic measurements made on two different days [1]. However, continuous measurement over a long period has been impossible due to severe environmental conditions.

Several recent measurements of ice sheet velocities used remotely sensed satellite data [2][3][4][5]. Use of optical sensor data is limited by cloud coverage and Sun elevation. SAR can provide frequently observed target data with high spatial resolution because it observes the ground surface in almost all weather conditions. An interferometric SAR (InSAR) technique to measure the movements of glaciers or ice sheets has been widely used because of its precise detection capability [3][4]. However, for glaciers with the greatest flow velocities such as the Shirase Glacier, the movement between two observations is generally too great to detect phase differences. Although image correlation can

determine flow velocity, any speckle noise on a SAR image impedes use of this technique.

This paper reports our preliminary results in ice-flow velocity estimation for the Shirase Glacier using correlation of images with the European Remote Sensing satellite-2 (ERS-2) data. First we introduced the procedure for measuring ice-flow velocities with image correlation. Next, we showed an example of ice-flow velocities of the Shirase Glacier determined by our proposed method. Finally, we analyzed and discussed the resulting ice flow velocity as predicted by our method.

II. SAR DATA AND IMAGE GENERATION

In this analysis we used the C-band SAR data acquired by the ERS-2. We needed an X-band downlink station to receive the observed data sent directly from the satellite within the station mask because ERS-2 does not have an onboard recorder to store the data for downloading outside the ground station mask. Syowa Station, a Japanese Antarctic research station located at S69.0 and E39.6, has been receiving the X-band data from ERS-2 since 1998. After sending the data in D1 cassettes back to Japan, the recorded raw data are usually processed and stored at the Japan Aerospace Exploration Agency's (JAXA's) Earth Observation Center (EOC).

We acquired the ERS-2 data from 2000 and 2002 for our analysis. Table 1 specifies the data used. We received all data processed in Level 0 and started our analysis at SAR image generation. We must resolve a Doppler frequency ambiguity before azimuth compression because ERS-2 has not been acquiring data in a yaw-steering mode since January 2001 due to a malfunction in its attitude control system. To remove these ambiguities in doppler frequencies, we determined the satellite's yaw angle from the doppler center frequency estimated from the raw data. After completing range compression and four multi-look process in azimuth compression, we transformed the slant-range data into ground-range coordinates. The pixel spacing of ground-range data is 12.5 m in both range and azimuth directions. The SAR image-generation software used in this analysis (Ongul SAR processor) was developed by one of the authors.

III. IMAGE CORRELATION PROCESS

The method we use for image correlation is based on the area-matching algorithm. Since the SAR data have relatively

high noise levels due to speckle noise compared with the optical sensor data, the following procedure is derived from our trial-and-error process.

A. Coarse matching

To reduce the noise level in the coarse-matching process, we averaged 16 samples, corresponding to 4 samples in azimuth by 4 samples in range, and created low-resolution images. We selected sets of tie points and derived quadratic transformation functions that convert master-image coordinates to slave-image coordinates by using the area-matching technique with the low-resolution images.

Because an important role of the coarse-matching process is to derive the geometric relation between master and slave images at geometrically fixed points, tie points at moving objects should be rejected in calculating the transform functions. When there is a great difference between the address calculated from transformation function and the actual address derived by matching procedure, the set of tie points is rejected in updating the transformation function.

The final transformation function is the relation of fixed points between master and slave images. Fig. 2 is an example of tie points selected in our coarse-matching process. This figure proves that most of the selected tie points are geometrically fixed points, such as rocks or unchanged coast lines.

B. Fine matching

Candidate selection for tie points is first applied in the fine-matching process to reduce matching errors caused by mismatched points. In our tie-point selection procedure, we used a texture variance \mathbf{S}_T^2 [6], calculated by the following equation, to select tie-point candidates on the master image.

$$\mathbf{S}_T^2 = \frac{\frac{\mathbf{S}^2}{n} - \frac{\mathbf{m}^2}{n}}{1 + \frac{1}{n}} \quad (1)$$

In this equation, \mathbf{m} and \mathbf{S} denote the mean and the standard deviation of pixel intensities within the image local window, and n is the equivalent number of looks of SAR data. The pre-setting threshold of \mathbf{S}_T determines tie points in the master image.

We calculated an address on the slave image (X_{s0}, Y_{s0}) that corresponds to the address on the master image (X_m, Y_m) using the results of the coarse-matching process, and extracted a search area on the slave image centered at the address (X_{s0}, Y_{s0}). To reduce speckle noise, we filtered data in both reference and search images. We used a Lee filter [7] with a 5×5 moving window in this process. After determining an integer address on the slave image, we interpolated both master and slave images using an FFT, zero-padding method,

then performed matching processes again on the interpolated image to determine the final address on the slave image (X_s, Y_s).

Although fine-matching processes are applied to all tie-point candidates, the matched points that have lower correlations are rejected as mismatched points.

C. Ice-flow calculation at matched points

After performing the processes as described in sections III. A and III. B, we calculated an ice flow velocity (v) and its direction (d) at the matched points in the slave image as follows.

$$v = \frac{\sqrt{(x_{ps}(X_s - X_{s0}))^2 + (y_{ps}(Y_s - Y_{s0}))^2}}{T_p} \quad (3)$$

$$d = \tan^{-1}\left(\frac{y_{ps}(Y_s - Y_{s0})}{x_{ps}(X_s - X_{s0})}\right) \quad (4)$$

In this equation, x_{ps} and y_{ps} indicate pixel spacing in azimuth and range directions, T_p is the time period between two datatakes. Fig. 3 summarizes the proposed procedure for glacier ice-flow estimation.

IV. ESTIMATED RESULTS OF GLACIERFLOW

We conducted a trial estimate of flow velocities for the Shirase Glacier using a series of ERS-2 data with either 35- or 70-day intervals, as listed in Table 1. The accumulation area is an inland area greater than 500 m in altitude and is covered by dry snow all year. Since the backscattering intensity of dry snow is consistently low, the inland area generally produces much lower texture information. As a result, the inland area also produces a lot of mismatched points in the matching process and gives us less reliable results. After screening these mismatched points using a defined threshold in correlation coefficients, the correctly matched points are sparsely located in the final image.

Fig. 4 shows an example of the derived ice flow velocities overlaid on the ERS-2 amplitude image. We can confirm the portions of the Shirase Glacier where we were able to determine stable flow velocities. As shown in Fig. 4, the areas where flow velocities could be determined are generally centered on crevasses and icebergs. Fig. 5 shows the changes in ice flow velocities in 2000 and 2002.

V. SUMMARY

We successfully used image correlation with SAR data to estimate the ice flow velocity of the Shirase Glacier. By using the proposed method, we derived ice flow velocities in areas that could not be estimated by the previously used InSAR technique. The next step of our study will be to apply our methods to the archived Japanese Earth Resources-1 (JERS-1) SAR data to derive past changes in ice flow velocities. This

detailed analysis is essential to determine the relation between flow velocities and other environmental data. We also plan to apply our method to SAR data available in the future, such as ALOS/PALSAR.

REFERENCES

- [1] Y. Fujii, "Aerophotographic interpretation of surface features and estimation of ice discharge at the outlet of the Shirase drainage basin," *Antarctica, Antarctic Record*, Vol. No.72, pp.1-15, 1981.
- [2] E. Berthier, B. Raup, and T. Scanbos, "Did the Mertz ice stream experience a velocity change during the last decade?," *Journal of Glaciology*, in press.
- [3] T. Scanbos, J. Bohlander, B. Raup, and T. Haran, "Velocity, Mass Balance, and Morphology of the Institute Ice Stream," *Antarctic Science*, in press.
- [4] E. Rignot and S. J. Stanley, "Rapid bottom melting widespread near Antarctic ice sheet grounding lines," *Science*, 296 (5575), pp. 2020-2023, 2002.
- [5] E. Rignot, D. G. Vaughan, M. Schmelts, T. Dupont, and D. MacAyeal, "Acceleration of Pine Island and Thwaites Glaciers, West Antarctica," *Ann. Glaciol.*, 34, pp. 189-194, 2002.
- [6] F. T. Ulaby, R. K. Moore and A. K. Fung, "Microwave remote sensing : Active and Passive, Vol. III," Artech House, Norwood, MA, 1986.
- [7] J. S. Lee, "Refined filtering of image noise using local statistics," *Computer Graphics Image Processing*, vol. 15, pp. 380-389, 1981.

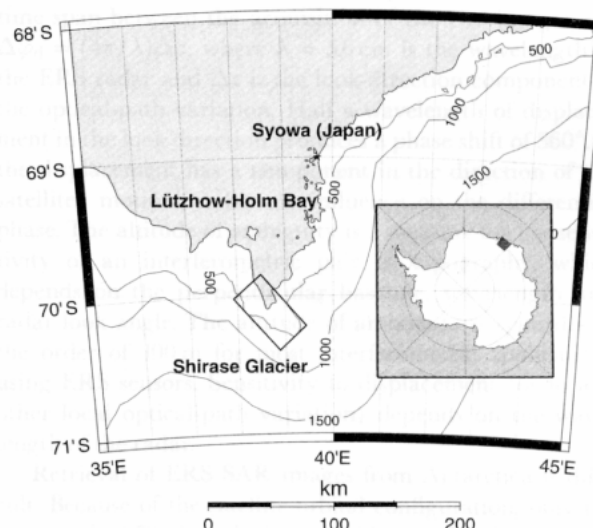


Fig. 1 Location of the Shirase Glacier.

Table 1 List of ERS-2 data used in the analysis.

Acquisition date	Orbit
2000/01/04	24608
2000/03/14	25610
2000/04/18	26111
2000/05/23	26612
2000/06/27	27113
2002/04/23	36632
2002/07/02	37634
2002/08/06	38135
2002/09/10	38636
2002/10/15	39137
2002/12/24	40139

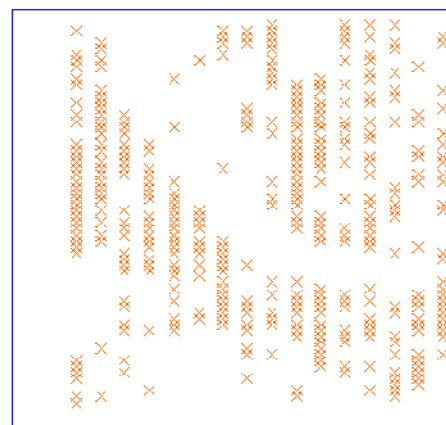


Fig. 2 Example of tie points selected in the coarse-matching process.

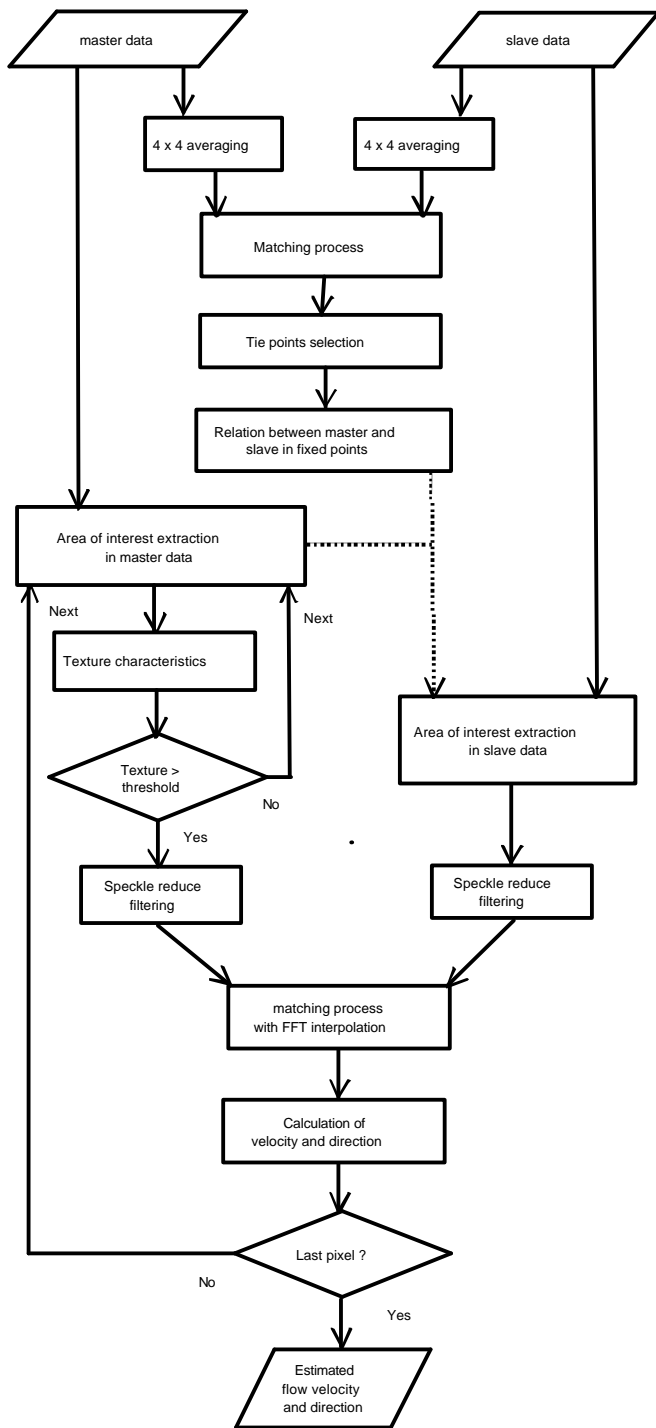


Fig. 3 Proposed procedure to determine glacier flow.

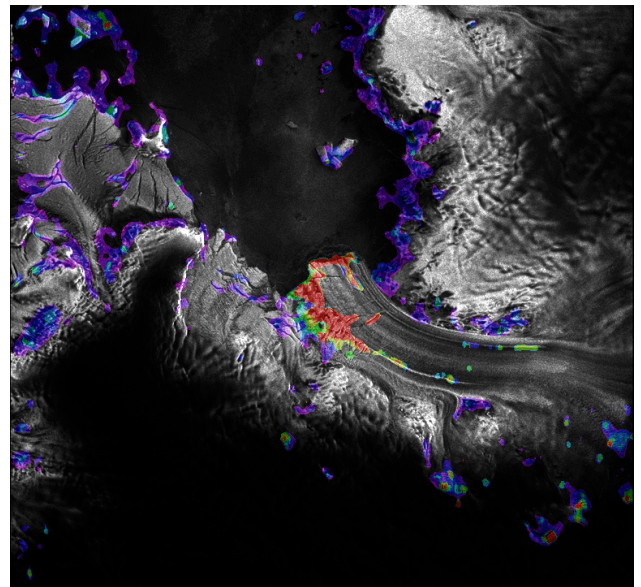


Fig. 4 Colorized areas are the portions of the Shirase Glacier where the flow-velocities are reliably calculated.

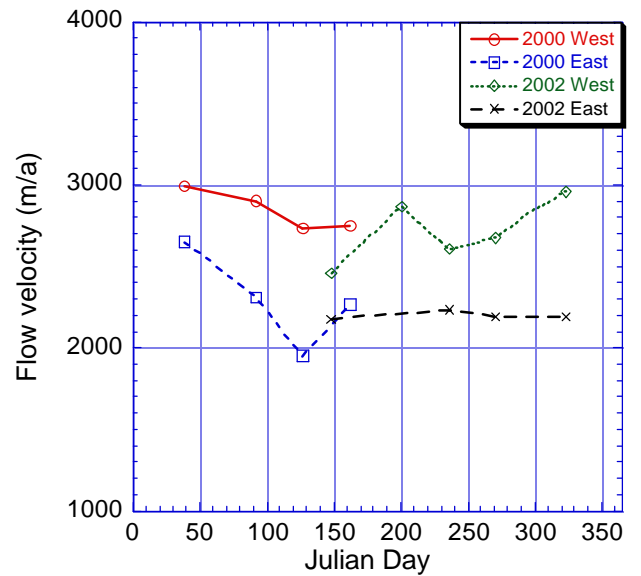


Fig. 5 Change of flow-velocities in 2000 and 2002.